Auxiliary Material Submission for Paper 2013GB004620

Reconciling the differences between top-down and bottom-up estimates of nitrous oxide emissions for the US Corn Belt

Timothy J Griffis (Department of Soil, Water, and Climate, University of Minnesota, Saint Paul, Minnesota, USA), Xuhui Lee (School of Forestry and Environmental Studies, Yale University, New Haven, Connecticut, USA), John M. Baker (USDA-ARS and Department of Soil, Water, and Climate, University of Minnesota, Saint Paul, Minnesota, USA), Michael P. Russelle (USDA-ARS and Department of Soil, Water, and Climate, University of Minnesota, Saint Paul, Minnesota, USA), Xin Zhang (Woodrow Wilson School of Public and International Affairs, Princeton University, Princteon New Jersey, USA), Rod Venterea (USDA-ARS and Department of Soil, Water, and Climate, University of Minnesota, Saint Paul, Minnesota, USA), and Dylan B. Millet (Department of Soil, Water, and Climate, University of Minnesota, Saint Paul, Minnesota, USA)

Griffis, T.J., X. Lee, J.M. Baker, M.P. Russelle, X. Zhang, R. Venterea, and D.B. Millet, Reconciling the differences between top-down and bottom-up estimates of nitrous oxide emissions for the US Corn Belt, Global Biogeochemical Cycles, XX, XXXX-XXXX

Introduction

This file provides additional details related to the bottom-up nitrous oxide emission calculations, the tall tower nitrous oxide concentration and flux measurements, nitrous oxide flux measurements from automated chambers, and other literature values of nitrous oxide emissions.

1. Auxiliary_Information_GBC_2013.doc. This word file describes the methodological details related to the bottom-up nitrous oxide emission estimates and the tall tower nitrous oxide concentration and flux measurements.

2. TableS1.doc. This word document (Table S1) is to be included within the Auxiliary_Information_GBC_2013.doc. This Table describes estimated synthetic nitrogen fertilizer, livestock populations, and manure-derived nitrogen for the Corn Belt.

3. FigureS1.pdf. This figure (Figure S1) is to be included with the Auxiliary_Information_GBC_2013.doc. This Figure compares the nocturnal boundary layer budget estimate of CO2 flux with eddy covariance CO2 fluxes.

4. FigureS2.pdf. This figure (Figure S2) is to be included with the Auxiliary_Information_GBC_2013.doc. This Figure shows the nighttime concentration footprint estimate for the tall tower based on the Stochastic Time-inverted Lagrangian Transport (STILT) model.

5. FigureS3.pdf. This figure (Figure S3) is to be included with the Auxiliary_Information_GBC_2013.doc. This Figure shows the wavelet decomposition for nitrous oxide concentration measurements at the Rosemount tall tower and for other “background” sites.

6. FigureS4.pdf. This figure (Figure S4) is to be included with the Auxiliary_Information_GBC_2013.doc. This Figure shows the influence of wind direction and air temperature on the tall tower nitrous oxide concentrations measured at 100 m above the ground.

7. FigureS5.pdf. This figure (Figure S5) is to be included with the Auxiliary_Information_GBC_2013.doc. This Figure shows the mean monthly nitrous oxide flux estimates based on four boundary-layer budget techniques.

8. FigureS6.pdf. This figure (Figure S6) is to be included with the Auxiliary_Information_GBC_2013.doc. This Figure shows the hourly soil nitrous oxide fluxes measured using an automated chamber system coupled to a tunable diode laser system in a corn/soybean agricultural field.

Reconciling the differences between top-down and bottom-up estimates of nitrous oxide emissions for the US Corn Belt

Timothy J. Griffis[1], Xuhui Lee[2,3], John M. Baker[1,4], Michael Russelle[1,4], Xin Zhang[5], Rod Venterea[1,4], Dylan Millet[1]

1. Department of Soil, Water, and Climate, University of Minnesota-Twin Cities

2. School of Forestry and Environmental Studies, Yale University

3. Yale-NUIST Center on Atmospheric Environment, Nanjing University of Information Science and Technology, Nanjing, China

4. United States Department of Agriculture – Agricultural Research Service

5. Woodrow Wilson School of Public and International Affairs, Princeton University, Princeton New Jersey, USA

Authors for correspondence:

Tim Griffis
Email: timgriffis@umn.edu
Phone: 612.625.3117

Xuhui Lee
Email: xuhui.lee@yale.edu
Phone: 203.432.6047

Auxiliary Information

1. Nitrogen inputs

We estimated nitrogen (N) inputs for the Corn Belt based on recent N use and sales statistics provided by the United States Department of Agriculture, Economic Research Service [USDA-ERS, 2011]. For the purpose of N accounting based on sales statistics, we define the Corn Belt by those states with significant corn/soybean land use. These states include: Illinois, Indiana, Iowa, Minnesota, Missouri, Ohio, South Dakota, and Wisconsin. The total area is estimated at 148 million ha. Here agriculture represents approximately 40% of the land use – similar to that in the vicinity of the Minnesota tall tower. These data have been summarized in Table S1. Approximately 5.0 Tg of synthetic N was added to the Corn Belt in 2010. The most significant source was associated with corn production.

An extensive survey of fertilizer use for the State of Minnesota determined that the average N application rate for corn was 157 kg ha^{-1} (140 lbs $acre^{-1}$) with a range of 145 to 164 kg ha^{-1} [Bierman et al., 2012]. This rate is in excellent agreement with our estimates for the entire Corn Belt. The patterns of fertilizer application (timing, amount, type) are important for driving bottom-up emission estimates and understanding the patterns of N_2O flux. For Minnesota, the most common fertilizer types were anhydrous ammonia and urea. Results from the fertilizer survey revealed that 45.9% of land managers used anhydrous ammonia while 44.8% used urea. Further complexity is introduced in terms of the timing of nitrogen application, which varies depending on N source and region. In general, anhydrous ammonia was applied 61% of the time in the fall and 28% of the time during spring. Urea was applied 75% during spring and about 10% during fall. The timing and type of N application can have an important impact on N_2O fluxes.

The major sources of biological N fixation (BNF) for the Corn Belt are derived from soybean and alfalfa. Typical rates of 84 kg N ha^{-1} and 152 kg N ha^{-1}, respectively have been reported for the Mississippi river basin [Russelle and Birr, 2004]. Our estimates for the Corn Belt based on the 8-digit HUC land use and yield information were 102 kg N ha^{-1} and 166 kg N ha^{-1}, respectively. Given the number of hectares planted for each of these crops, we estimated a combined BNF of 2.8 Tg N y^{-1}. Further, the amount of N added back to corn systems in the form of aboveground residue was estimated at 2.2 Tg N y^{-1}.

Using the most recent agricultural census data [USDA-NASS, 2009] we have estimated N inputs in the form of manure [Lorimor et al., 2004] for the Corn Belt (Table S1). Estimates of daily manure N rate per head of livestock were estimated for swine (17.7 kg N y^{-1}), cattle (57.9 kg N y^{-1}), sheep (6.6 kg N y^{-1}), turkey (1.6 kg N y^{-1}), layers (0.43 kg N y^{-1}), broilers (0.35 kg N y^{-1}) and horses (39.7 kg N y^{-1}). Given the estimated populations for each of these species, and assuming that manure is distributed evenly across the agricultural lands, we estimated an N application rate of 46.3 kg N ha^{-1} y^{-1} or 2.7 Tg N y^{-1}.

Finally, we considered N inputs in the form of wet and dry N deposition, using an average flux of 9.1 kg N ha^{-1} y^{-1}, 1.3 Tg N y^{-1}) [Anderson and Downing, 2006], and local re-deposition [Anderson and Downing, 2006; Burkhart et al., 2005] of N in the form of ammonium and ammonia (NH_x,12.3 kg N ha^{-1} y^{-1}, 1.8 Tg N y^{-1}).

Table S1. Estimated synthetic nitrogen fertilizer, livestock populations, and manure-derived nitrogen for the Corn Belt

2. Nocturnal Boundary Layer Budget of Carbon Dioxide

Figure S1: Comparison of the CO_2 nocturnal boundary layer budget and eddy covariance techniques. The solid line is a 7-day running mean of the NBL budget.

3. Nighttime N_2O Concentration Footprint

The nighttime (20:00 to 04:00 hour) concentration footprint was estimated using the Stochastic Time-inverted Lagrangian Transport (STILT) model using data for September 2009 [Lin et al., 2003]. With this analytical approach, we calculated the footprint for each hour by releasing 100 air parcels at the receptor (44º41'19"N, 93º04'22"W, 185 m) and transporting them backward for one night. The figure below shows the averaged footprint during the nighttime, and it indicates that the nighttime concentration measurement at 185 m is strongly influenced by sources within about 120 km of the tall tower.

Figure S2. Concentration footprint of the tall tower determined using the STILT model in September 2009. The color scale represents the log10 footprint, and the unit of the footprint is ppm (µmole m^{-2} s^{-1})$^{-1}$ (top panel). Cumulative percentage footprint contribution based on the nocturnal STILT analysis (bottom panel).

4. Spatio-temporal variability in N_2O Concentrations

Figure S3. Wavelet analysis of N_2O concentration from select "background" sites and the Rosemount tall tower (100 m level). The wavelet decomposition is used here to extract the seasonal variability (A5, middle panels) and the short-term (hourly) noise (D5, right panels).

Figure S4. Influence of wind direction and air temperature on the tall tower N_2O observations measured at the 100 m level.

5. Boundary Layer N_2O Budgets

The mean monthly N_2O emissions for each boundary layer budget technique are shown in Figure S5 and indicate that June, August, and September had the largest mean emissions. Overall, the largest fluxes were observed during the growing season, which is generally consistent with automated soil chamber measurements.

Figure S5: Mean monthly nitrous oxide flux estimates based on the nocturnal boundary layer (NBL), modified Bowen ratio (MBR night and daily), and equilibrium boundary layer (EBL) techniques for 2011. The dashed line shows the ensemble mean. The cross-correlation matrix shows a correlation ranging from 0.47 to 0.80 for the various methods.

6. Automated Soil Chamber N_2O Fluxes

Figure S6. Hourly soil N_2O fluxes measured using an automated chamber system coupled to a tunable diode laser.

7. Other N_2O sources

The upscaling calculations required estimates of other N_2O sources within the footprint of the tall tower. These were based on literature values and included emissions from natural vegetation [Zhuang et al., 2012], urban land use [EDGAR V4.2], and lakes [McCrackin and Elser, 2010; McCrackin and Elser, 2011; Mengis et al., 1997].

8. References

United States Department of Agriculture – Economic Research Service, United States, Fertilizer use and price. *Technical report* 2011, 2011

Bierman P, Rosen C, Venterea R, Survey of nitrogen fertilizer use on corn in Minnesota. *Agricultural Systems* 109: 43–52, 2012

Russelle M, Birr A, Large-scale assessment of symbiotic dintorgen fixation by crops: Soybean and alfalfa in the Mississippi River Basin. *Agronomy Journal* 96: 1754-1760, 2004

United States Department of Agriculture – National Agricultural Statistics Service, Census of agriculture, 2007. *Technical Report* 2009, 2009

Lorimor J, Powers W, Sutton A, Manure characteristics: Manure management systems series, mwps-18, section 1, *Technical report*, Iowa State University, Midwest Plan Service, Iowa State University, Ames, Iowa, 2004

Anderson K, Downing J, Dry and wet atmospheric deposition of nitrogen, phosphorous and silicon in an agricultural region. *Water, Air, and Soil Pollution* 176: 351–374, 2006

Burkhart M, Liebman DJM, Herndl C, Impacts of integrated crop-livestock systems on nitrogen dynamics and soil erosion in western Iowa watersheds. *Journal of Geophysical Research-Biogeosciences* 110: G01009, doi:10.1029/2004JG000008, 2005

Zhuang Q, Lu Y, Chen M, An inventory of global N_2O emissions from the soils of natural terrestrial ecosystems. *Atmospheric Environment* 47: 66-75, 2012

McCrackin ML, Elser JJ, Atmospheric nitrogen deposition influences denitrification and nitrous oxide production in lakes. *Ecology* 91: 528-539, 2010

McCrackin ML, Elser JJ, Greenhouse gas dynamics in lakes receiving atmospheric nitrogen deposition. *Global Biogeochemical Cycles* 25: GB4005, 2011

Mengis M, Gachter R, Wehrli B, Sources and sinks of nitrous oxide (N_2O) in deep lakes. *Biogeochemistry* 38: 281-301, 1997

Table S1. Estimated synthetic nitrogen fertilizer, livestock populations, and manure-derived nitrogen for the Corn Belt

Crop	**Area (10^6 ha)**	**Rate (kg N ha^{-1})**	**Total N (Tg N y^{-1})**
Corn	24.6	142.6	3.5
Soybean	21.8	3.2	0.07
All wheat varieties	3.3	55.7	0.18
Cotton	0.12	77.2	0.009
Other	10.0	122.7	1.2
Total	**59.8**	**-**	**4.96**

Type	**Population (10^6)**	**Rate (kg N $animal^{-1}$)**	**Total N (Tg N y^{-1})**
Cattle	27.6	57.9	1.60
Swine	45.0	17.7	0.79
Sheep	1.2	6.6	0.008
Layers	146.5	0.43	0.06
Broilers	477.2	0.35	0.17
Turkey	46.5	1.6	0.07
Horses	0.85	39.7	0.03
Total	**744.9**	**-**	**2.74**

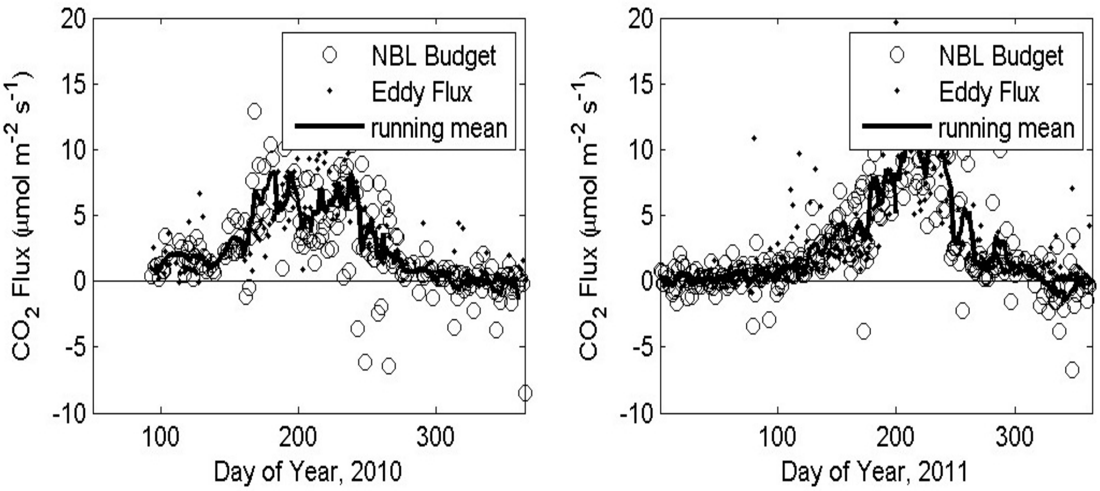

Figure S1: Comparison of the CO_2 nocturnal boundary layer budget and eddy covariance techniques. The solid line is a 7-day running mean of the NBL budget.

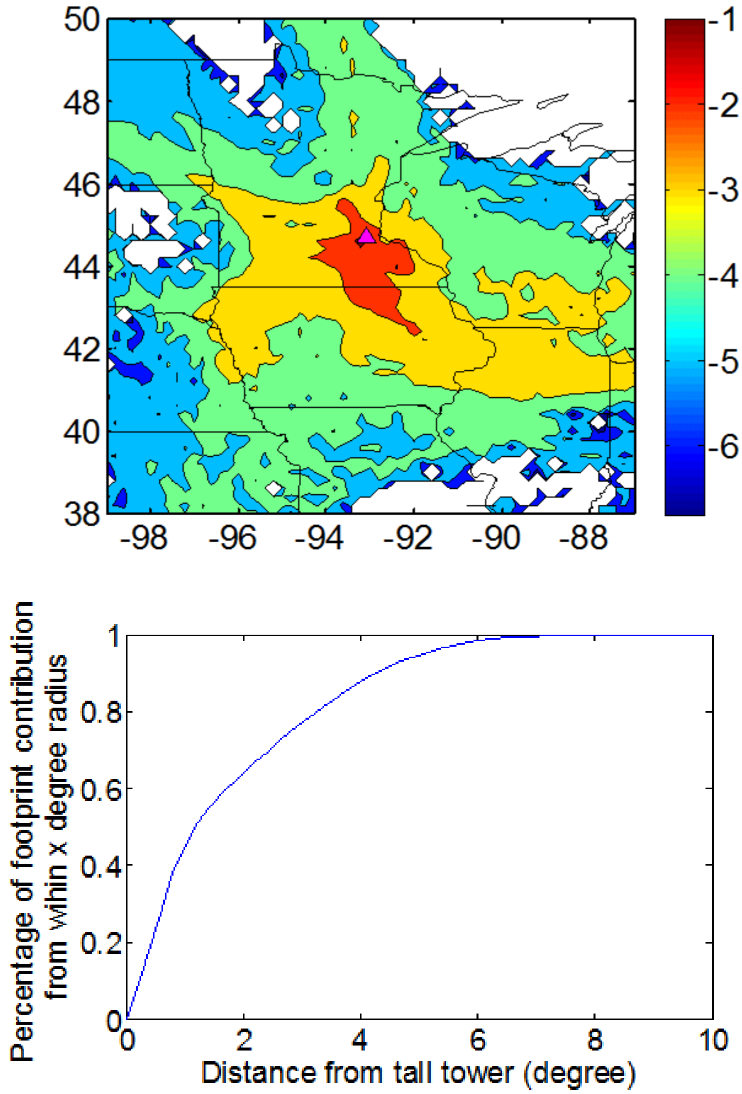

Figure S2. Concentration footprint of the tall tower determined using the STILT model in September 2009. The color scale represents the log10 footprint, and the unit of the footprint is ppm (μmole m^{-2} s^{-1})$^{-1}$ (top panel). Cumulative percentage footprint contribution based on the nocturnal STILT analysis (bottom panel).

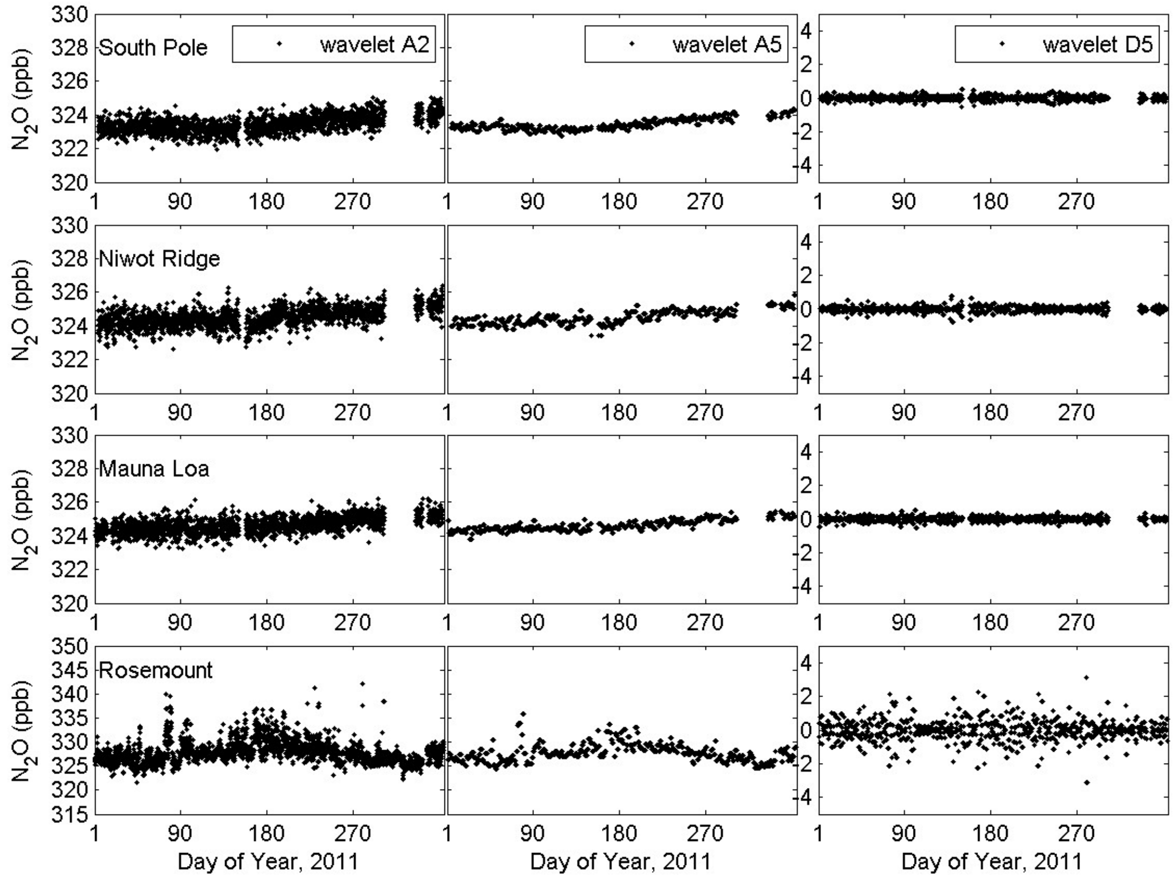

Figure S3. Wavelet analysis of N_2O concentration from select “background” sites and the Rosemount tall tower (100 m level). The wavelet decomposition is used here to extract the seasonal variability (A5, middle panels) and the short-term (hourly) noise (D5, right panels).

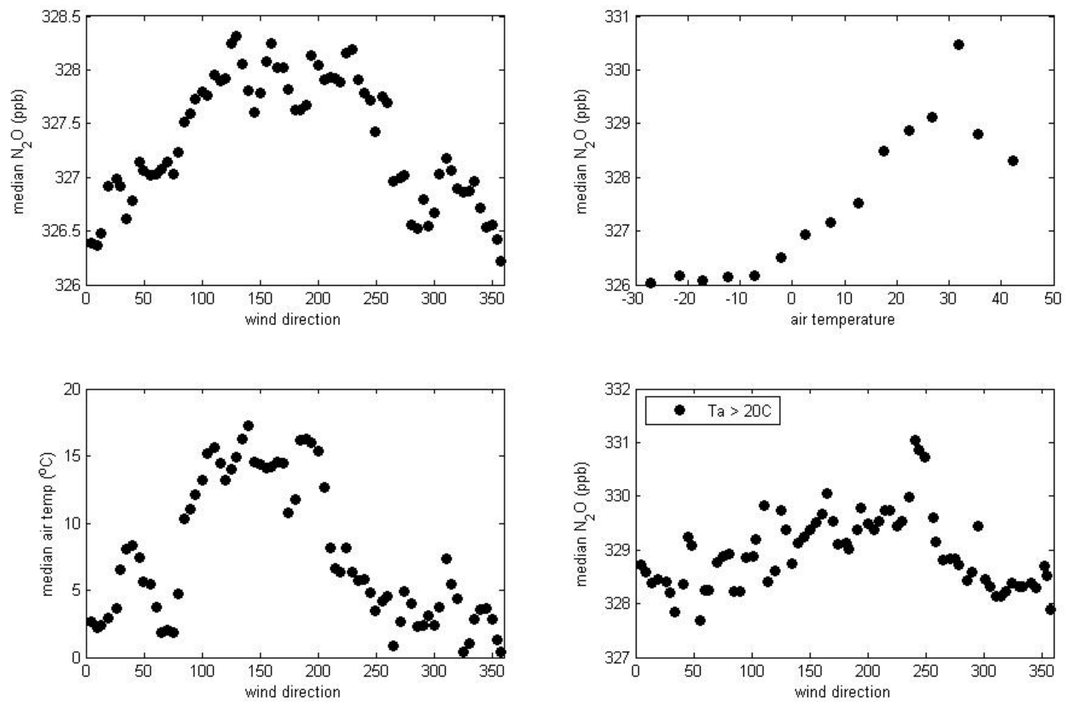

Figure S4. Influence of wind direction and air temperature on the tall tower N_2O observations measured at the 100 m level.

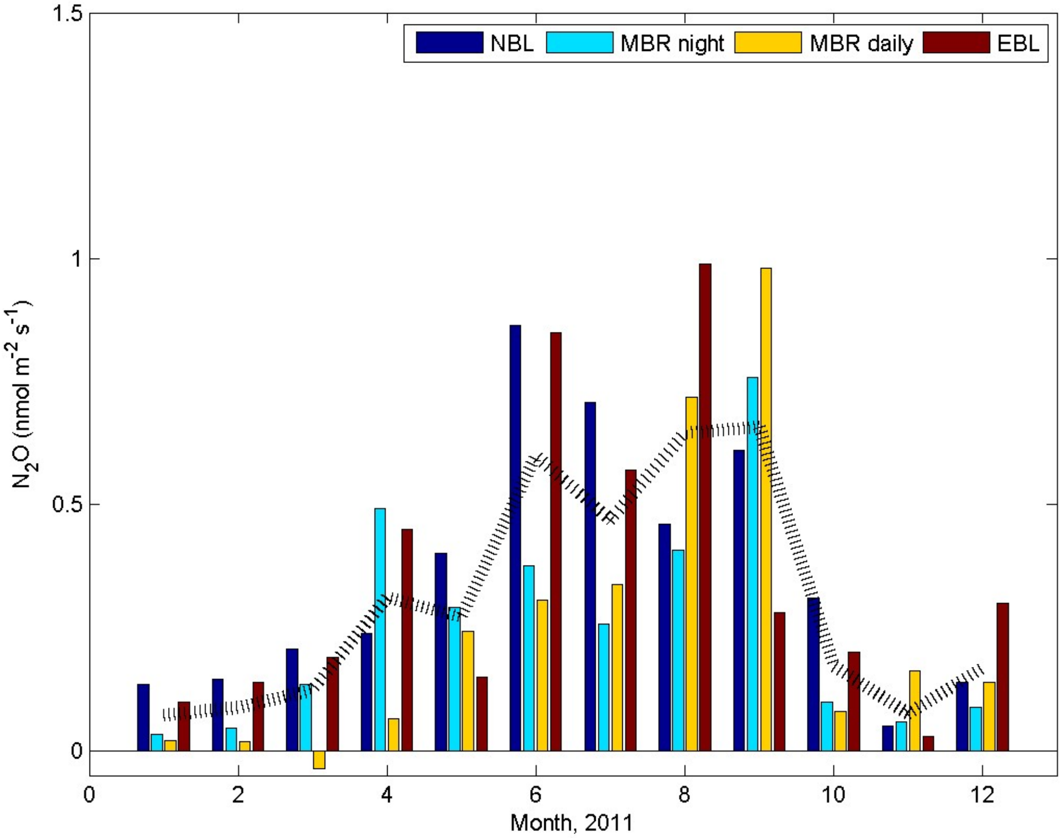

Figure S5: Mean monthly nitrous oxide flux estimates based on the nocturnal boundary layer (NBL), modified Bowen ratio (MBR night and daily), and equilibrium boundary layer (EBL) techniques for 2011. The dashed line shows the ensemble mean. The cross-correlation matrix shows a correlation ranging from 0.47 to 0.80 for the various methods.

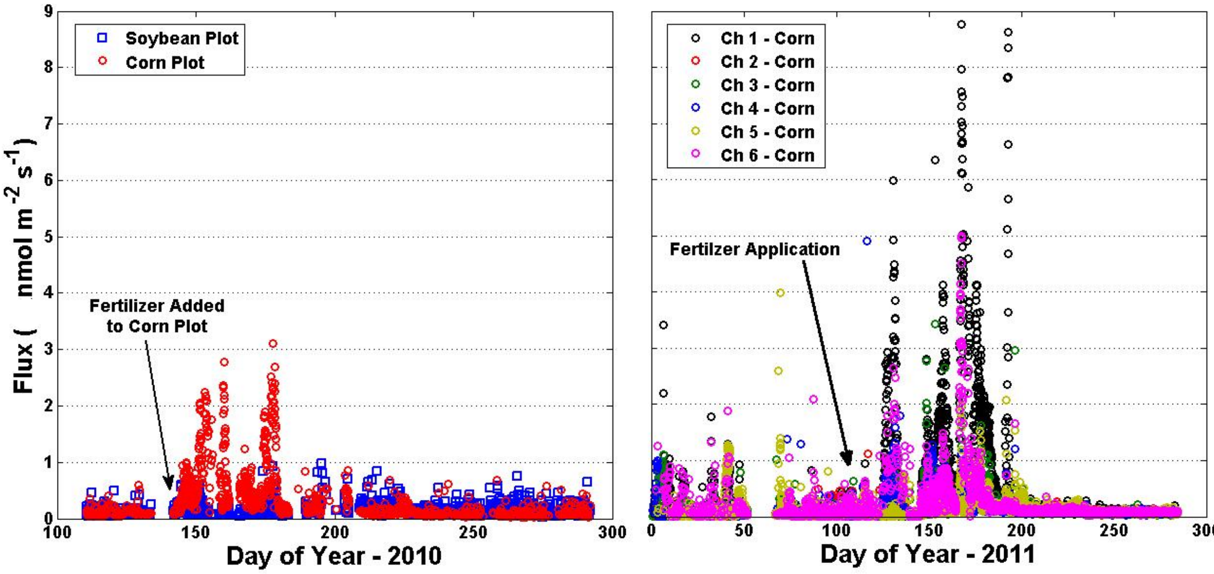

Figure S6. Hourly soil N_2O fluxes measured using an automated chamber system coupled to a tunable diode laser.